Comparison of two-phase and three-phase macroscopic models of equiaxed grain growth in solidification of binary alloy with electromagnetic stirring

Wang Tao, Engang Wang, Yves Delannoy, Yves Fautrelle, Olga Budenkova

Published after MCWASP XV 2020
by
IOP Publishing
In
IOP Conf. Series: Materials Science and Engineering **861** (2020) 012026
doi:10.1088/1757-899X/861/1/012026

Comparison of two-phase and three-phase macroscopic models of equiaxed grain growth in solidification of binary alloy with electromagnetic stirring

T Wang[1,2,4], S Semenov[3], E Wang[1,4], Y Delannoy[2], Y Fautrelle[2] and O Budenkova[2]

[1] Key Laboratory of Electromagnetic Processing of Materials (Ministry of Education), Northeastern University, P. R. China
[2] Univ. Grenoble Alpes, CNRS, Grenoble INP, SIMAP, F-38000 Grenoble, France
[3] On leave from Univ. Grenoble Alpes, CNRS, Grenoble INP, SIMAP, F-38000 Grenoble, France
[4] School of Metallurgy, Northeastern University, Shenyang 110004, P. R. China
olga.budenkova@grenoble-inp.fr

Abstract. Simulations of equiaxed solidification using two-phase and three-phase models are performed for the experimental benchmark AFRODITE with electromagnetic stirring. A three-phase model which was presented by authors elsewhere accounts for solid phase, inter- and extradendritic liquid phases. With respect to that model, the two-phase approach can be considered as reduced or simplified, yet, this implies also less number of assumptions regarding closure relations. One of parameters which exists in both models and which cannot be transposed directly from one model to another is critical packing fraction at which solid phase is supposed to be blocked. In simulations a large difference in evolution of convective flow and developement of the solid phase was found. As expected, final segregation obtained with two–phase model is stronger, yet, it is qualitatively similar to the segregation pattern obtained with three-phase model.

1. Introduction

In industrial casting production, a large equiaxed grain region is often expected because it is supposed to provide better homogeneity than the structure consisting of columnar grains [1]. Both industrial and laboratory experiments indicate that forced convection may promote formation of equiaxed grains. On the other hand, it is also known that the interaction between convection and solidifying structure may lead to appearance of channels, freckles and zones of macrosegregation. Yet, post-mortem analysis of sample provides information only about the final state of solidification which can be rather puzzling since its evolution in time remains unclear. As far as in-situ experiments are concerned, they often deal with rather weak convective flow because of a small thickness of the sample and the total size of the latter is rather small, therefore, these observations could not be easily transposed to large-scale solidification processes. Consequently, numerical modeling is needed to understand how the character of solid formation (columnar or equiaxed) affects convection and solute transport during solidification process. However, numerical simulation of solidification with equiaxed grains is more challenging than

of columnar ones because such phenomena as nucleation, grains' drag by liquid phase, and their packing due to interaction with walls and other grains have to be considered. Currently, volume averaged method makes simulation of equiaxed solidification under forced convection at macroscale possible [2]. However, despite the variety of existing equiaxed solidification models [3–7], reliablity of results of simulations remains largely uncertain because of following reasons. First, is that these models rely on various physical assumptions used to close system of equations and contain lots of empirical parameters to which numerical results are quite sensitive [8–13]. Second, there is a lack of experimental data which could help to validate model of solidification in a purely equiaxed regime in presence of convection. In such situation it is important to perform parametric studies and to compare results of calculations for same solidification problem using different parameters or closure relations or even results obtained with models based on different approaches. For example, in the simulation of 2.45 ton ingot solidification by Li et al. [9], it was found that the presence of equiaxed grains cause severe negative segregation at the bottom, however, if maximum nuclei density is larger than some critical value, the segregation will be relieved. With a simplified two-phase equiaxed model, Krane et al. [13] simulated a benchmark solidification case using different packing limit fraction. They concluded that for a two-phase model the packing limit fraction had to be very likely smaller than 0.637, which is the value traditionally used in three-phase model. Wang et al. [8] demonstrated crucial effect of solute diffusion length on the calculation results of macrosegregation in Hebditch-Hunt case using three-phase model. Wu et al. found that in solidification of Al–4.7 wt.% Cu alloy two-phase globular equiaxed model predicts heavier segregation than three-phase dendritic one. Plotkowski et al. [11] compared three different grain attachment models, that are constant packing fraction scheme, average solid velocity method and continuum attachment approach. The above studies help to understand the role of various parameters and assumptions in equiaxed solidification modeling, yet, none of reported studies used experimental results to validate their models.

Present works deals with comparison of three-phase and two-phase modeling of solidification in the equiaxed regime of a binary Sn-10%wt.Pb alloy under the action of electromagnetic convection. This modeling is based on experimental data issued from the experiment, referred hereafter as AFRODITE, which is briefly described below while details of the experiment and segregation pattern observed in the solidified sample can be found elsewhere [14]. Application of three-phase model to this experimental case using its simplied two-dimensional description was also reported previously [20]. In the present study we were interested if a two-phase model which can be considered reduced (or simplified) compared to three-phase provides similar results regarding grain growth, their motion and segregation pattern.

2. Description for solidification case

The experiment under consideration presents solidification of a binary Sn–10 wt.%Pb alloy in a rectangular cavity with inner size of 100×60×10 mm (Figure 1). In the experiment a constant difference of 40 K is imposed for temperatures at the heaters adjacent to the lateral walls of the cavity, and cooling rate of CR = 0.03 K/s is applied to solidify the sample [29], other walls are regarded as non-slip and adiabatic. Thermal resistance between heaters and cavity walls makes the temperature differences across the soldifiying volume smaller and corresponds to nearly 15 degrees [38] that was taken as conditions in calculations along with indicated cooling rate. A travelling magnetic field created with a linear motor placed horizontally along the cavity and below gave rise to Lorentz force $\vec{F}_{ems}$ acting mainly along the bottom and rapidly decreasing in the vertical direction. An analytical expression for the resulting Lorentz force presented in [30] was used in numerical simulations.

The AFRODITE experiment is supposed to be a quasi-2D benchmark although modeling performed for the case of a purely thermo-solutal convection showed that front and back walls of the cavity strongly affected flow. To reduce the problem from 3D to 2D an additional force was introduced into momentum equations [37]. In present case the flow is less intense and comparison of temperature field evolution obtained in two-dimensional simulations with that registered in the experiment shows similarities, i.e. flow calculated in two-dimensions represent the real one at the large extent without insertion of any

additional forces in the equation. Furthermore, simulations of the melt flow performed with laminar approach, both for 2D and 3D configurations, showed instabilities and did not converge because of the interaction of two vortices existing in the fluid. One of the vortex appears because of the electromagnetic stirring, yet, the force flow cannot overcome the thermal convection near the hotter boundary. Consequently, for further simulations a realizable k-ε turbulent model was used. It was found that value of the calculated turbulent viscosity was rather low that indicated weak turbulence.

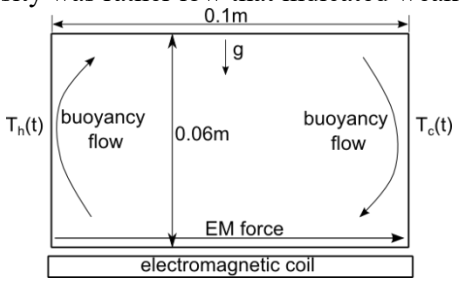

Figure 1. Scheme of the experimental set-up. Condition $T_h(t)$-$T_c(t)$=15^{0}C is used in simulations

3. Model description

The shape of equiaxed grain depends on cooling condition and grain size. In principal, equiaxed grains prefer to grow with globular shape when their sizes are still small [7]. In most conditions, the equiaxed grains will transit from globular shape to dendritic one due to the faster increase of tip velocity than diffusion-controlled growth velocity [3]. In present work, similar to other models [5,21], we assume dendritic shape for three-phase model and globular shape for two-phase mode (Figure 2). In three-phase model, the liquid phase have to be divided into inter- and extradendritic parts. The interdendritic liquid in the model is united with solid dendrites thus giving grain phase within an envelope. Details of three-phase model can be found elsewhere [8,20], below only a two-phase model is shortly presented.

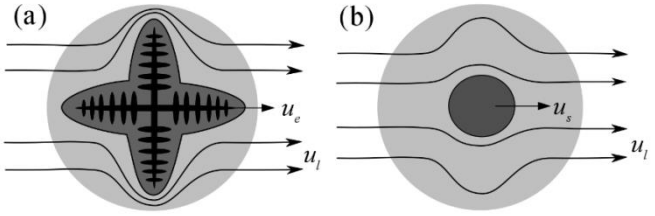

Figure 2. Schematic figure of an equiaxed grain with dendritic shape (a) and globular solid grain (b).

The two-phase model described above has similar system of equations and solution algorithm as previously reported three-phase model [8], governing equations are presented in Table 1 with differences in growth model presented also in the Table 2. In two-phase model, the volume fraction of solid phase f_s and liquid phase f_l , satisfy the constraint $f_s + f_l = 1$. Both phases have their proper velocities v_l and v_s, temperatures T_l and T_s, and concentrations of the solute c_l and c_s. Initial state of the model is supposed to be pure melt of a nominal concentration c_0, whose temperature is above the liquidus temperature. With condition of thermal equilibrium between solid and liquid phases, an infinitely fast heat transfer between the phases is assumed which is provided in the model with a large value of heat transfer coefficient (Table 1). Once the constitutional undercooling somewhere in the volume is larger than critical value, the nucleation happens with the nucleation rate N_Φ giving rise to grains number density (concentration of grains) n. It is supposed that nucleation can happen throughout the process if liquid fraction exists, conditions of constitutional undercooling are satisfied and total number of grains is below of maximal one defined with n_{max}. Although assumption regarding importance of dendrites' fragmentation as a source of nuclei can be found elsewhere [22], this phenomenon is not taken into account in the models presented here to limit uncertainty of the latter. Further the transport equation is solved for n thus defining the local number of grains which is related to the size of grains. It is supposed

that n is transported with the velocity of the solid phase whose small amount appears simultaneously with nucleation and whose growth occurs according to local undercooling, i.e. to the distribution of the concentration in surrounding liquid. In the vicinity of grain the latter is defined by convective transport but also by diffusion of the solute rejected by the solid phase according to the phase diagram. Similar to [7] and based on our experience [8] we suppose that the solute diffusion length becomes smaller because of liquid flow around the grain. The back diffusion in solid is neglected. The shrinkage phenomenon due to phase transition and cooling is neglected, i.e. all densities in the conservation equations are constant and equal to the reference density: $\rho_l = \rho_s = \rho_{ref}$. Similar to Založnik and Combeau [5], to model the sedimentation (here the floating) phenomenon, in the buoyancy term, a constant difference between the solid phase density and a reference density is introduced. The Boussinesq approximation accounts for solutal and thermal convection in the liquid phase.

Table 1. Conservation equations, source terms, and auxiliary expressions

1. Conservation equations	
Mass	$\frac{\partial(f_l\rho_l)}{\partial t} + \nabla(f_l\rho_l\vec{u}_l) = M_{sl} - M_\Phi$ $\qquad$ $\frac{\partial(f_s\rho_s)}{\partial t} + \nabla(f_s\rho_s\vec{u}_s) = M_{ls} + M_\Phi$
Momentum	$\frac{\partial(f_l\rho_l\vec{u}_l)}{\partial t} + \nabla(f_l\rho_l\vec{u}_l\vec{u}_l) = -f_l\nabla p + \nabla[\mu_l f_l(\nabla\vec{u}_l + (\nabla\vec{u}_l)^{\mathrm{T}})] + \vec{u}_l M_{sl} + \vec{F}_{Bl} + \vec{U}_{el}^D + \vec{F}_{ems}$
	$\frac{\partial(f_s\rho_s\vec{u}_s)}{\partial t} + \nabla(f_s\rho_s\vec{u}_s\vec{u}_s) = -f_s\nabla p + \nabla[\mu_s f_s(\nabla\vec{u}_s + (\nabla\vec{u}_s)^{\mathrm{T}})] + \vec{u}_l M_{ls} + \vec{F}_{Bs} + \vec{U}_{ls}^D + \vec{F}_{ems}$
Energy	$\frac{\partial(f_l\rho_l h_l)}{\partial t} + \nabla(f_l\rho_l\vec{u}_l h_l) = \nabla(k_l f_l\nabla T) + LM_{ls}f_l + M_{sl}h_l + Q_{sl}$
	$\frac{\partial(f_s\rho_s h_s)}{\partial t} + \nabla(f_s\rho_s\vec{u}_s h_s) = \nabla(k_s f_s\nabla T) + LM_{ls}f_e + M_{ls}h_l + Q_{ls}$
	where $h_l = \int_{T_{ref}}^{T_l} c_p^l dT + h_l^{ref}$, $h_s = \int_{T_{ref}}^{T_s} c_p^s dT + h_s^{ref}$
Solute	$\frac{\partial(f_l\rho_l c_l)}{\partial t} + \nabla(f_l\rho_l\vec{u}_l c_l) = \nabla(D_l f_l\nabla c_l) + J_{sl}$ $\qquad$ $\frac{\partial(f_s\rho_s c_s)}{\partial t} + \nabla(f_s\rho_s\vec{u}_s c_s) = J_{ls}$
Grain number density	$\frac{\partial}{\partial \mathrm{t}} n + \nabla(\vec{u}_s n) = N_\Phi$
2. Source terms	
Mass	$M_{ls} = -M_{sl} = \rho_l \cdot S_s \cdot v_{env}$, $\qquad$ $M_\Phi = N_\Phi\rho_l \cdot \frac{1}{6}\pi d_0^3$
Momentum	$\vec{F}_{Bl} = f_l\rho_l\vec{g}\left[\beta_T(T_{ref} - T_l) + \beta_c(c_{ref} - c_l)\right]$, $\qquad$ $\vec{F}_{Bs} = f_s(\rho_s^b - \rho_{ref})\vec{g}$
	$\vec{U}_{ls}^D = -\vec{U}_{sl}^D = K_{ls}(\vec{u}_l - \vec{u}_s)$
Energy	$Q_{ls} = -Q_{sl} = H^*(T_l - T_s)$, $H^* = 1 \times 10^9\ W\ m^{-3}K^{-1}$
Solute	$J_{le} = -J_{el} = (M_{ls} + M_\Phi) \cdot c_s^*$
Grain number density	$N_\Phi = \begin{cases} f_l(n_{max} - n)/\Delta t, & \Delta T > \Delta T_{nucl}\ or\ n < 1 \\ 0, & else \end{cases}$

Auxiliary expressions

$c_l^* = \frac{T_l - T_0}{m}$, $\qquad$ $c_s^* = k \cdot c_l^*$, $\qquad$ $v_{ls} = \frac{D_l}{l_l} \cdot \frac{c_l^* - c_l}{c_l^* - c_s^*}$, $\qquad$ $S_s = f_l \cdot (36\pi \cdot n)^{1/3} \cdot f_s^{2/3}$

$K_{ls} = \begin{cases} 4f_l^2\beta^2\frac{\mu_l}{d_s^2} & f_s < f_p^s \\ \frac{180\mu_l f_s^2}{f_l d_s^2} & f_s > f_p^s \end{cases}$ $\qquad$ $l_l = \frac{d_s}{2}\left(\frac{1}{1-f_s^{\frac{1}{3}}} + \frac{Sc^{\frac{1}{3}}Re^a}{3f_l}\right)^{-1}$ $\qquad$ $\beta = \left\{\frac{9}{2}f_s\frac{2+\frac{4}{3}f_s^{\frac{5}{3}}}{2-3f_s^{\frac{1}{3}}+3f_s^{\frac{5}{3}}-2f_s^2}\right\}^{1/2}$

To calculated the drag force in two-phase model we use Happel model [24] for a low solid fraction and when grains are packed the Kozeny-Carman model [25] is applied. Note that in three-phase model the approach is similar but the drag force is calculated with grain fraction since it is applied to grains. Regarding grains packing, we choose to block those grains whose fraction is above a critical one and which are situated either near the wall or near already packed neighboring grain. This allows us to avoid unphysical situation with blocking of grains brought to the cavity center by forced convection.

The main differences between the models are in phase transition mechanism with accompanying transport phenomena, in kinematic interaction between the phases and in treatment of grain packing. In three-phase model the growth of solid phase is related to growth of grains, which is described as expansion of an imaginary envelope, but not in a straightforward manner. Rejection of solute happens at the solid-liquid interface toward interdendritic liquid and its further transport to the extrandendritic liquid occurs via molecular diffusion but is also affected by growth of grains. In two phase model, the phase transition occurs directly between the liquid and solid phase and liquid phase transit to solid phase directly. In the three-phase model the packing is applied to grains while solid fraction inside can be rather small, i.e. the region of interdenritic liquid can be large. In two-phase model the phase which is packed is the solid phase that means that to have similar situation with large amount of liquid between solid the packing has to be performed earlier. It is widely accepted that the packing fraction limit for the grain phase is 63.7% [10,12,26], which is an approximation of the closest packing fraction of randomly arranged monodisperse spheres. However, when accounting for dendritic structure, the limit for solid phase is lower and accepted to be in the range $f_p^s = 0.1{\sim}0.5$ [13,27,28]. In present simulations two-phase model a value of $f_p^s = 0.3$ is defined for packing limit fraction while in three-phase model the critical value still is $f_p^{\mathrm{e}} = 0.637$.

Table 2. Phase transfer rate between phases in models

Conservative quantities	Two phase model $l \to s$	Three phase model	
		$l \to d$	$d \to s$
Surface area concentration	$S_s = f_l \cdot (36\pi \cdot n)^{\frac{1}{3}} \cdot f_s^{\frac{2}{3}}$	$S_{\mathrm{e}} = f_l \cdot (36\pi \cdot n)^{\frac{1}{3}} \cdot f_e^{\frac{2}{3}}$	$S_{\mathrm{ds}} = f_e \cdot \rho_s \cdot \frac{2 \cdot f_d^e}{\lambda_2}$
Interface movement velocity	$v_{ls} = \frac{D_l}{l_l} \cdot \frac{c_l^* - c_l}{c_l^* - c_s^*}$	$v_{env} = \Phi_M \frac{D_l \cdot m_l \cdot (\kappa - 1) \cdot c_l^*}{\pi^2 \cdot \Gamma} \cdot \left[\frac{(c_l^* - c_l)}{c_l^*(1-k)}\right]^2$	$v_{ds} = \frac{D_l}{l_d} \cdot \frac{c_l^* - c_d}{c_l^* - c_s^*}$
Phase transfer rate	$M_{ls} = S_s \cdot v_{ls}$	$M_{ld} = S_e \cdot v_{env}$	$M_{ds} = S_{ds} \cdot v_{ds}$

Note: $\Phi_{\mathrm{M}} = 0.683$ is growth shape factor assuming an octahedral grain envelope shape[10].

4. Results and discussion

To understand results presented below it should be reminded that in the model the density of the solid phase in the buoyancy term is smaller than the density of liquid and that this differences increases with enrichment of the fluid by rejected solute. This means that growing grains float in the liquid instead of been sediment. Simulations start with overheated liquid in order to have the temperature and flow field installed before solidification is started. Consequently, first nuclei appear nearly at 180s of calculations at the upper corner of the colder boundary, at the right side in the presented configuration. The solid (in 2-phase model) and equiaxed (in 3-phase model) phase which starts to appear is brought rapidly to the center of the cavity where it is remelted. Solidification along the whole colder wall begins at ~400s of calculations. Then, the grains which appear closer to the bottom part first travel in the cold zone along the wall that allow them to grow till the fraction at which they can be blocked (packed) and some of them can travel along the upper wall without been remelted. Since that time the solid grains in two-phase model and equiaxed grains in three-phase model start to fill the cavity.

After 540s of calculations time temperature fields obtained in two-phase and three-phase models are different because of difference in convective flow (Figure 3 (a) and (b)). In two-phase model most of grains are located at the top of the cavity, moreover, the packed grains completely occupy the upper boundary and damp the convective flow there (Figure 3 (a) and (c)). The forced flow caused by electromagnetic stirring exists along the colder wall of the cavity and in its lower part where fraction of the solid phase is low. Because of a stronger forced convection the temperature field is more perturbed and a region of low temperature appears in the bottom half of the cavity. Also, forced convection defines transport of rejected solute, a part of which is captured in the center of its vortex. In three-phase model two vortexes with different direction exist in the cavity. The vortex generated by Lorentz force is located only at a lower half and a vortex due to thermal-solute effect occupies the upper half of the cavity (Figure 3b). While equiaxed grains present almost everywhere in the volume the solid fraction is actually grows only at the colder side and the packing zone is located there.

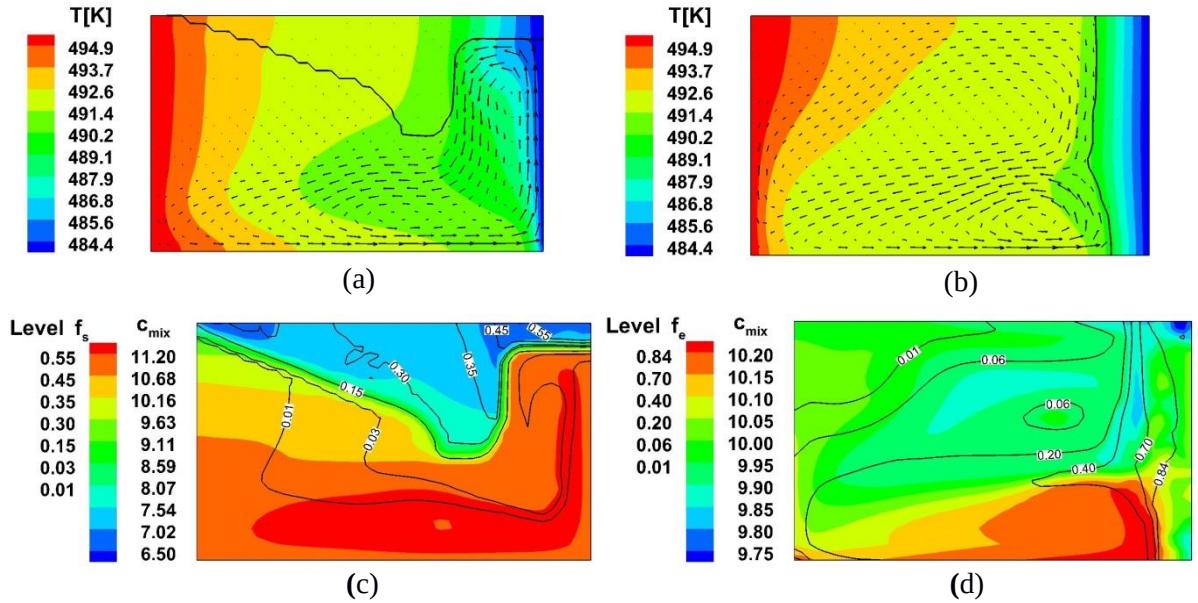

Figure 3. Results obtained at 540s of simulations: temperature distribution in two-phase (a) and three-phase (b) model, the black line on these picture correspond to the edge of the zone of packed grains defined with f_s=0.3 in two-phase model and f_e=0.637 in three-phase model, velocity field in the liquid is superposed over temperature distribution; map of the average concentration and contours for solid fraction in two-phase model (c) and grain fraction for three-phase model (d).

Final macrosegregation maps obtained with two models are shown in Figure 4, both models show negative segregation at the top, in two-pahse model the value of segregation is much more pronounced.

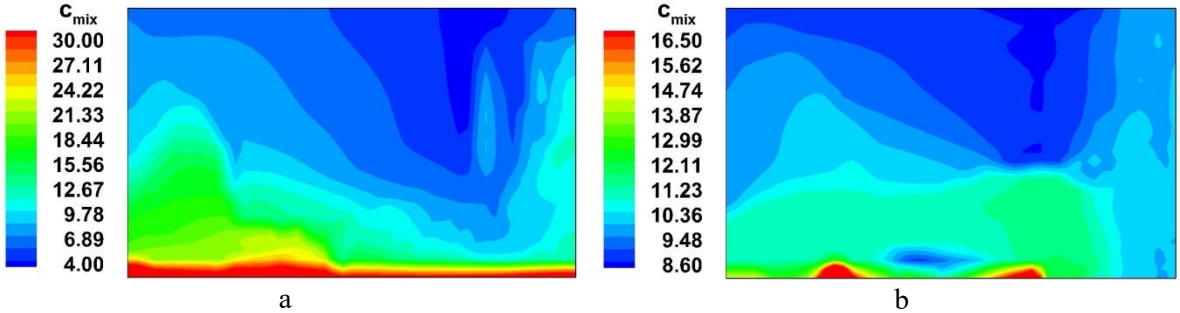

Figure 4. Final macrosegregation map obtained with two-phase (a) and three-phase (b) model.

In both models the positive segregation forms in the lower part of the cavity and in both cases it is extended almost over the whole bottom wall. In three-phase model the zone of segregation has a more compact form which is more similar to the experimental results (see Figure 12 (c) in [17]).

Based on results of simulations formation of both, positive and negative segregation zones is quite easy to explain. At early stage of solidification the solid grains are brought to the top by forced convection and also due to their less density compared to that of the liquid. They solidify taking less value of solute and rejecting the excess to the liquid which becomes even more heavier. Rejected solute is captured by the forced convection which brings it to the bottom but also drag upward slightly. At the same time heavier fluid tends to sediment throughout the process and mostly at the final stage of solidification, when the grains are packed yet liquid (extradendritic in three-phase model) continues to move between them.

An interesting phenomenon which cannot be presented here because of a short format of the paper is the interaction of forced and buoyancy flow which is responsible for the shape of the zone of negative segregation at the upper part of the cavity.

5. Summary

A two-phase and three-phase equiaxed solidification models are applied to simulations of AFRODITE experiment on solidification of a binary Sn–10 wt.%Pb alloy under the forced convective flow driven by electromagnetic force. Simulations show that with chosen set of parameters both models provide qualitatively similar results which resemble final distribution of Pb in the sample obtained via X-Ray imaging. Analysis of results show that fraction at which grains are getting packed is one of the crucial parameters since it defines regions of action of forced and buoyancy convection in the case under consideration. Evolution of the convective flow is different in two models because it is subjected to the interaction with solid phase (in two-phase model) and grain phase (in three-phase). Different flow field leads to different temperature evolutions during the process. Surprisingly, despite these differences throughout the process, calculated final macrosegregation maps shows qualitatively similar results. In both cases negatively segregated layer at top is formed and positive segregation zone is observed at bottom similar to the experimental case. This indicates probably that final segregation is largely defined by residual flow through rigid solid network.

Acknowledgements

This work is a joint cooperation between the SIMAP laboratory of Grenoble INP (France) and the Key Laboratory of EPM of Northeastern University (P. R. China). The authors gratefully acknowledge financial support from the National Nature Science Foundation of China (Grant No. U1760206), the National Key R&D Program of China (Grant No. 2017YFE0107900), the Project of Introducing Talents of Discipline Innovation to Universities 2.0 (the 111 Project of China 2.0, No. BP0719037). The SIMAP laboratory acknowledges the financial support provided by the ESA-MAP MICAST project contract 14347/01/NL/SH.

References

[1] Wang F, Wang E, Zhang L, Jia P and Wang T 2017 *J. Manuf. Process.* **26** 364–71
[2] Wu M, Ludwig A and Kharicha A 2019 *Metals (Basel).* **9** 229
[3] Wu M and Ludwig A 2009 *Acta Mater.* **57** 5621–31
[4] Ni J and Beckermann C 1993 *J. Mater. Process. Manuf. Sci.* **2** 217–31
[5] Založnik M and Combeau H 2010 *Comput. Mater. Sci.* **48** 1–10
[6] Wang C Y and Beckermann C 1996 *Metall. Mater. Trans. A* **27** 2754–64
[7] Appolaire B, Combeau H and Lesoult G 2008 *Mater. Sci. Eng. A* **487** 33–45
[8] Wang T, Semenov S, Wang E, Delannoy Y, Fautrelle Y and Budenkova O 2019 *Metall. Mater. Trans. B* **50** 3039-3054
[9] Li J, Wu M, Ludwig A and Kharicha A 2014 *Int. J. Heat Mass Transf.* **72** 668–79
[10] Wu M and Ludwig A 2009 *Acta Mater.* **57** 5632–44

[11] Plotkowski A and Krane M J M 2017 *Metall. Mater. Trans. B* **48** 1636–51
[12] Leriche N, Combeau H, Gandin C A and Založnik M 2015 *IOP Conf. Ser. Mater. Sci. Eng.* **84** 1–8
[13] Krane M J M 2004 *Appl. Math. Model.* **28** 95–107
[14] Wang X and Fautrelle Y 2009 *Int. J. Heat Mass Transf.* **52** 5624–33
[15] Fautrelle Y, Wang X D, Hachani L, Saadi B and Zaidat K 2015 *Int. J. Therm. Sci.* **91** 34–48
[16] Hachani L, Saadi B, Wang X D, Nouri A, Zaidat K, Belgacem-Bouzida A, Ayouni-Derouiche L, Raimondi G and Fautrelle Y 2012 *Int. J. Heat Mass Transf.* **55** 1986–96
[17] Hachani L, Zaidat K and Fautrelle Y 2015 *Int. J. Heat Mass Transf.* **85** 438–54
[18] Hachani L, Zaidat K and Fautrelle Y 2016 *Int. J. Therm. Sci.* **110** 186–205
[19] Hachani L, Zaidat K, Saadi B, Wang X D and Fautrelle Y 2015 *Int. J. Therm. Sci.* **91** 34–48
[20] Wang T, Wang E, Delannoy Y, Fautrelle Y and Budenkova O 2019 *IOP Conference Series: Materials Science and Engineering* vol 529 p 12030
[21] Ludwig A and Wu M 2002 *Metall. Mater. Trans. A* **33** 3673–83
[22] Zheng Y, Wu M, Kharicha A and Ludwig A 2017 *Model. Simul. Mater. Sci. Eng.* **26** 15004
[23] Wu M, Ludwig A, Bührig-Polaczek A, Fehlbier M and Sahm P R 2003 *Int. J. Heat Mass Transf.* **46** 2819–32
[24] Happel J 1958 *AIChE J.* **4** 197–201
[25] Bird R B, Stewart W E and Lightfoot E N 1960*Transport Phenomena John Wiley and Sons* (NY)
[26] Jiang D and Zhu M 2017 *Metall. Mater. Trans. B* **48** 444–55
[27] Plotkowski A and Krane M J M 2016 *Appl. Math. Model.* **40** 9212–27
[28] Olmedilla A, Založnik M, Messmer T, Rouat B and Combeau H 2019 *Phys. Rev. E* **99** 12907
[29] Boussaa R, Hachani L, Budenkova O, Botton V, Henry D, Zaidat K, Ben Hadid H and Fautrelle Y 2016 *Int. J. Heat Mass Transf.* **100** 680–90
[30] Wang X, Moreau R, Etay J and Fautrelle Y 2009 *Metall. Mater. Trans. B* **40** 104–13
[31] Založnik M, Kumar A and Combeau H 2010 *Comput. Mater. Sci.* **48** 11–21
[32] Stankus S V. and Khairulin R A 2006 *High Temp.* **44** 389–95
[33] Plevachuk Y, Sklyarchuk V, Yakymovych A, Willers B and Eckert S 2005 *J. Alloys Compd.* **394** 63–8
[34] Wang C Y and Beckermann C 1993 *Metall. Mater. Trans. A* **24** 2787–802
[35] Ciobanas A I and Fautrelle Y 2007 *J. Phys. D. Appl. Phys.* **40** 3733–62
[36] Wang C Y, Ahuja S, Beckermann C and de Groh H C 1995 *Metall. Mater. Trans. B* **26** 111–9
[37] Botton V, Boussaa R, Debacque R, Hachani L, Zaidat K, Ben Hadid H, Fautrelle Y and Henry D 2013 *Int. J. Therm. Sci.* **71** 53–60
[38] Zheng Y, Wu M, Karimi-Sibaki E, Kharicha A and Ludwig A 2018 *Int. J. Heat Mass Transf.* **122** 939–53